

Giant suppression of the Drude conductivity due to quantum interference in disordered two-dimensional systems

G. M. Minkov,¹ A. V. Germanenko,² O. E. Rut,² A. A. Sherstobitov,¹ and B. N. Zvonkov³

¹*Institute of Metal Physics RAS, 620219 Ekaterinburg, Russia*

²*Institute of Physics and Applied Mathematics, Ural State University, 620083 Ekaterinburg, Russia*

³*Physical-Technical Research Institute, University of Nizhni Novgorod, 603600 Nizhni Novgorod, Russia*
(Dated: September 18, 2018)

Temperature and magnetic field dependences of the conductivity in heavily doped, strongly disordered two-dimensional quantum well structures GaAs/In_xGa_{1-x}As/GaAs are investigated within wide conductivity and temperature ranges. Role of the interference in the electron transport is studied in the regimes when the phase breaking length L_ϕ crosses over the localization length $\xi \sim l \exp(\pi k_F l/2)$ with lowering temperature, where k_F and l are the Fermi quasimomentum and mean free path, respectively. It has been shown that all the experimental data can be understood within framework of simple model of the conductivity over delocalized states. This model differs from the conventional model of the weak localization developed for $k_F l \gg 1$ and $L_\phi \ll \xi$ by one point: the value of the quantum interference contribution to the conductivity is restricted not only by the phase breaking length L_ϕ but by the localization length ξ as well. We show that just the quantity $(\tau_\phi^*)^{-1} = \tau_\phi^{-1} + \tau_\xi^{-1}$ rather than τ_ϕ^{-1} , where $\tau_\phi \propto T^{-1}$ is the dephasing time and $\tau_\xi \sim \tau \exp(\pi k_F l)$, is responsible for the temperature and magnetic field dependences of the conductivity over the wide range of temperature and disorder strength down to the conductivity of order $10^{-2} e^2/h$.

PACS numbers: 73.20.Fz, 73.61.Ey

I. INTRODUCTION

It is commonly accepted that all states are localized in two-dimension (2D) systems at arbitrary disorder.¹ The localization length at zero magnetic field can be estimated as²

$$\xi \simeq l \exp(\pi k_F l/2), \quad (1)$$

where l is the mean free path and k_F is the Fermi quasimomentum. This result was obtained for noninteracting electrons at zero temperature. Another characteristic length which appears at finite temperature is a phase breaking length, L_ϕ . Just the ratio between these characteristic lengths determines the conductivity regime.

When $\xi \gg L_\phi$ one can consider electrons as delocalized ones. The conductivity, σ , in this regime can be well described starting with the classical Drude model. When the quantum effects are ignored, the conductivity is given by the Drude formula

$$\sigma_0 = e^2 n \tau / m = \pi G_0 k_F l, \quad (2)$$

where $G_0 = e^2/(2\pi^2 \hbar)$, n is the electron density, τ and m are the transport relaxation time and electron effective mass, respectively. Two quantum corrections to the conductivity determine both the temperature and magnetic field dependences of the conductivity at low enough temperature when the electron gas is degenerated and phonon scattering does not influence the momentum relaxation. They are the weak localization (WL) or interference correction and the correction caused by the electron-electron (e - e) interaction. The WL correction is negative and logarithmically increases in magnitude with the decreasing temperature when the spin relaxation is

absent. The interaction correction, as a rule, is also negative and increases in absolute value with the lowering temperature if the gas parameter r_s is less than unity and the system is in the diffusion regime, $T\tau \ll 1$ (hereafter we set $\hbar = 1$, $k_B = 1$). Thus, the conductivity at $\xi \gg L_\phi$ decreases with T -decrease and remains significantly higher than G_0 .

In opposite case, $\xi \ll L_\phi$, the electrons can be considered as well localized. The conductivity in this regime is hopping and should be described in framework of the percolation theory.³ The conductivity under this condition is significantly less than G_0 .

Thus, the range of the conductivity values, where both approaches are wrong in the strict sense, is very wide. For example, an unusual metallic-like temperature dependence of the conductivity is experimentally observed just within this range.^{4,5} A crossover from the weak to strong localization or, by other words, the crossover from conductivity over delocalized states to the conductivity over localized states takes place also here.

In order to avoid possible misunderstanding we would like to note at the very beginning that throughout this paper we will use terms “conductivity over *delocalized* states” and “conductivity over *localized* states” in the following senses. The conductivity over *delocalized* states means that one can describe the transport phenomena (the temperature, magnetic- and electric-field dependences of the longitudinal and transverse conductivity) starting from the model of free electrons. The incoherent and coherent scattering and the e - e interaction are taken into account as perturbation. Just for this case the quantitative expressions for temperature and magnetic field dependences of the conductivity was obtained.^{6,7,8,9,10,11}

The term “conductivity over *localized* states” means

that one has to describe the transport phenomena starting from the model of well localized states, considering the transitions between them as perturbation. This approach holds when the “conductivity” between two nodes in the equivalent Miller-Abrahams network is significantly less than the conductivity quantum e^2/h . Taking into account the disorder, the conductivity of the whole network is relatively small, $\sigma \ll e^2/h$.

Experimentally, the conductivity of 2D systems at $\sigma \lesssim G_0$ was studied in the number of papers.^{12,13,14,15,16,17,18} In most cases the data are interpreted from the position of the hopping mechanism of the conductivity. The expressions obtained in framework of the percolation theory are widely used for quantitative analysis. Only in Refs. 14 and 17 it is pointed out that some of the dependences look like that for the conductivity over delocalized states.

As mentioned above, the crossover from weak to strong localization is governed by the ratio ξ/L_ϕ . That is why, it would be interesting to trace the changing of the temperature and magnetic field dependences of the conductivity and Hall effect at continuous variation of the ξ to L_ϕ ratio. There are two different ways for that. It can be done by varying either the disorder strength (i.e., ξ) or the temperature (i.e., L_ϕ). The first can be realized on structures of different design. For example, centrally doped quantum well structures, the structures with remote doping layers, the structures of different doping level, or the gated structures can be investigated. However, the electron density and mobility change simultaneously in this way.

The second way, the changing of the temperature, seems more suitable because all the parameters remain constant except L_ϕ . Strongly disordered (with small τ -value) 2D system with electron gas of high density is appropriate object in this case. Strong disorder ensures that the interference correction, which is proportional to $\ln(\tau_\phi/\tau)$, is comparable in magnitude with the Drude conductivity at $k_F l > 1$ at accessibly low temperatures. The high electron density and low mobility guarantee the degeneracy of the electron gas and negligibility of the phonon scattering up to the relatively high temperature. Thus, changing the temperature it is possible to cross over from the regime $L_\phi > \xi$ to the regime $L_\phi < \xi$ keeping disorder unchanged. Just this line of attack is used in Refs. 19 and 20 to study the crossover from weak to strong localization in quasi-one-dimensional structures.

In this paper, we present the results of experimental study of the temperature and magnetic field dependences of the conductivity and Hall effect in the heavily δ -doped quantum well GaAs/In_xGa_{1-x}As/GaAs structure within wide temperature range.

II. SAMPLES

We have investigated two heterostructures, 4261 and 4262, which are distinguished by doping level. They were

grown by metal-organic vapor-phase epitaxy on a semi-insulating GaAs substrate and consist of 0.5- μm -thick undoped GaAs epilayer, a 80- \AA In_{0.2}Ga_{0.8}As quantum well with Sn δ layer situated in the well center and a 2000- \AA cap layer of undoped GaAs. The tin density, N_δ , in δ layer was about $2 \times 10^{12} \text{ cm}^{-2}$ and $1 \times 10^{12} \text{ cm}^{-2}$ for structure 4261 and 4262, respectively. Several samples were mesa etched from each wafer into standard Hall bars and then an Al gate electrode was deposited onto the cap layer by thermal evaporation. The measurements were performed in the temperature range 0.4 – 80 K at magnetic field B up to 6 T. The electron density at $V_g = 0$ was $1.8 \times 10^{12} \text{ cm}^{-2}$ in the structure 4261 and $0.9 \times 10^{12} \text{ cm}^{-2}$ in the structure 4262. Since the results were mostly analogous for both structures, we restrict our attention in this paper to the structure 4261 only.

III. RESULTS AND DISCUSSION

To characterize the structures investigated, Fig. 1(a) shows the gate voltage dependence of the Hall density, $n_H = 1/(eR_H)$, measured at $T = 77 \text{ K}$ when the interaction correction to the Hall coefficient is negligible. One can see that the electron density linearly depends on the gate voltage with the slope $dn_H/dV_g = 3.5 \times 10^{11} \text{ cm}^{-2}\text{V}^{-1}$ which accords well with the structure design and capacitance measurements. Fig. 1(b) shows the electron-density dependences of the conductivity at $T = 77 \text{ K}$ and $T = 4.2 \text{ K}$. Already this figure shows that the change of the conductivity with temperature is strong for the relatively high electron density. So the conductivity difference for these temperatures is about one order of magnitude for $n \simeq 5 \times 10^{11} \text{ cm}^{-2}$ (the Fermi energy, E_F , is about 20 meV).

To clarify the role of the quantum corrections at low conductivity when $k_F l \simeq 1.5 - 2$ let us analyze the exper-

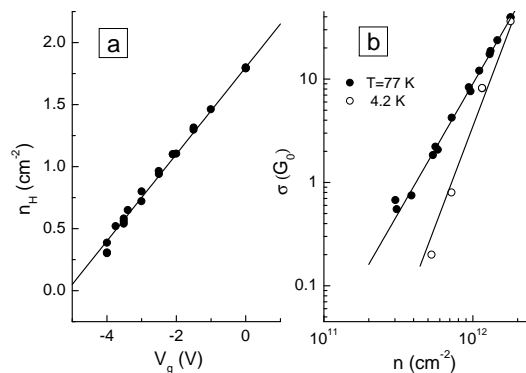


FIG. 1: (a) – The gate-voltage dependence of the Hall density $n_H = 1/(eR_H)$ for $T = 77 \text{ K}$. Symbols are the experimental results. Straight line is drawn with the slope $dn/dV_g = 3.5 \times 10^{11} \text{ cm}^{-2}\text{V}^{-1}$. (b) – The conductivity in zero magnetic field for two temperatures as a function of electron density. Symbols are the experimental results. Lines are provided as a guide to the eye.

imental data starting from the case of $k_F l \gg 1$ when the conventional theories of the quantum corrections work beyond question. We will not present all data and restrict ourselves by the cases of the key $k_F l$ -values: (i) the minimal $k_F l$ -value when we do not observe a deviation from the conventional theories of the quantum corrections yet; (ii) the case of the maximal $k_F l$ -value where deviations are already evident; (iii) the minimal $k_F l$ -value when we are able to understand all the dependences after some modification of the conventional theory which takes into account the partial localization of the electron wave function and, at last, (iv) the case when a new approach for description of the conductivity is required from our point of view.

Let us begin with the analysis of the data obtained at $V_g = -2.1$ V, $n = 1.1 \times 10^{12}$ cm $^{-2}$ that corresponds to the first case. Fig. 2(a) shows the temperature dependence of the conductivity at $B = 0$. One can see that the σ -vs- T dependence is close to the logarithmic one over the whole temperature range. The low-magnetic-field dependences of the conductivity $\sigma = \rho_{xx}^{-1}$ measured in the temperature range from 1.6 K to 40 K are shown in Fig. 2(b). As evident the magnetoresistance demonstrates the typical features corresponding to the suppression of weak localization by magnetic field: the temperature decrease leads to the sharpening of the minima at $B = 0$.

To treat the data quantitatively one needs to know the values of the Drude conductivity σ_0 . As seen from Fig. 2(a) the change of the conductivity with the temperature increase for such disordered systems is strong already for relatively high conductivity. The conductivity is enhanced in magnitude more than fifty percent in our temperature range. Therefore, there are difficulties in determination of σ_0 . We use the procedure analogous to that described in Refs. 17 and 21. It allows us to obtain simultaneously the values both of σ_0 and of τ_ϕ .

The conductivity in the absence of a magnetic field can be written as

$$\sigma(T) = \sigma_0 + \delta\sigma^{WL}(T) + \delta\sigma_b^{WL}(T) + \delta\sigma_{ee}(T). \quad (3)$$

Here, $\delta\sigma^{WL}(T)$ and $\delta\sigma_b^{WL}(T)$ stand for the backscattering²² and non-backscattering¹¹ parts of the interference quantum correction, respectively. In the diffusion regime, $\tau \ll \tau_\phi$, they are

$$\delta\sigma^{WL}(T) = \beta G_0 \ln \left[\frac{\tau}{\tau_\phi(T)} \right], \quad \delta\sigma_b^{WL} = G_0 \ln 2, \quad (4)$$

where β is equal to unity.²¹ The last term in Eq. (3) is the quantum correction caused by the e - e interaction. For $T\tau \ll 1$, it reads^{23,24,25,26}

$$\begin{aligned} \delta\sigma_{ee}(T) &= \left\{ 1 + 3 \left[1 - \frac{\ln(1 + F_0^\sigma)}{F_0^\sigma} \right] \right\} G_0 \ln T\tau \\ &\equiv K_{ee} G_0 \ln T\tau. \end{aligned} \quad (5)$$

where F_0^σ is the Fermi-liquid constant. The interaction correction has been studied for analogous quantum-well

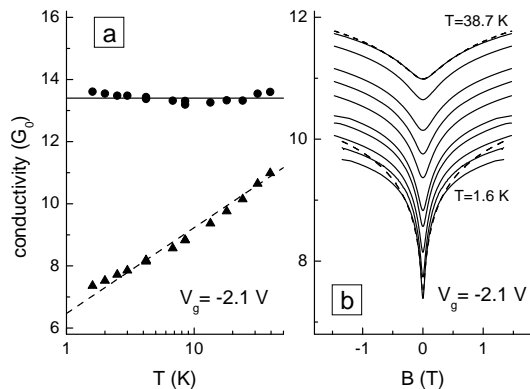


FIG. 2: (a) – The temperature dependence of the conductivity at $B = 0$ for $V_g = -2.1$ V. The values measured experimentally are shown by triangles. Circles are the Drude conductivity found experimentally for the different temperatures as described in text. Solid line is $\sigma_0 = 13.4 G_0$. Dashed line is the dependence $1.2 \ln T$. (b) – The magnetic-field dependence of the conductivity measured for different temperatures: $T = 38.7, 31.0, 23.5, 17.7, 13.2, 8.5, 6.8, 4.2, 2.5,$ and 1.6 K (from top to the bottom). Solid lines are experimental, dashed lines are example of the fit by Eq. (6) carried out for $T = 1.6$ K and 38.7 K within the magnetic field range from $-0.3 B_{tr}$ to $0.3 B_{tr}$, $B_{tr} \simeq 1.25$ T.

structure in our previous papers.^{17,27} In particular, it has been observed experimentally²⁷ that K_{ee} starts to decrease below $k_F l \sim 4$ and apparently tends to zero with further lowering $k_F l$. Close behavior is demonstrated in the structures investigated in this paper; K_{ee} practically vanishes when $k_F l \lesssim 2$. The theoretical explanation of this fact may possible require going to the next order in disorder in Finkel'stein's renormalization-group scheme.²³ Presenting the values of K_{ee} for each concrete case, we will not discuss this issue in this paper anymore.

The shape of the low-field negative magnetoconductance $\Delta\sigma(B) = \rho_{xx}^{-1}(B) - \rho_{xx}^{-1}(0)$, caused by the suppressing interference correction is described by the Hikami-Larkin-Nagaoka (HLN) expression^{6,8}

$$\begin{aligned} \Delta\sigma(B) &= \alpha G_0 \mathcal{H} \left(\frac{\tau}{\tau_\phi}, \frac{B}{B_{tr}} \right), \\ \mathcal{H}(x, y) &= \psi \left(\frac{1}{2} + \frac{x}{y} \right) - \psi \left(\frac{1}{2} + \frac{1}{y} \right) - \ln x, \end{aligned} \quad (6)$$

where $B_{tr} = \hbar/(2el^2)$ is the transport magnetic field, $\psi(x)$ is a digamma function, and α is the prefactor. With taking into account two-loop correction and interplay of weak localization and interaction, the prefactor α should depend on the conductivity as follows^{21,28}

$$\alpha = 1 - \frac{2G_0}{\sigma}, \quad \sigma > 2. \quad (7)$$

Expressions from (3) to (6) have been used to find σ_0 and τ_ϕ . We used a successive approximation method as in Ref. 17. For the first approximation we have set σ_0 equal to the experimental value σ at $B = 0$, found seed values

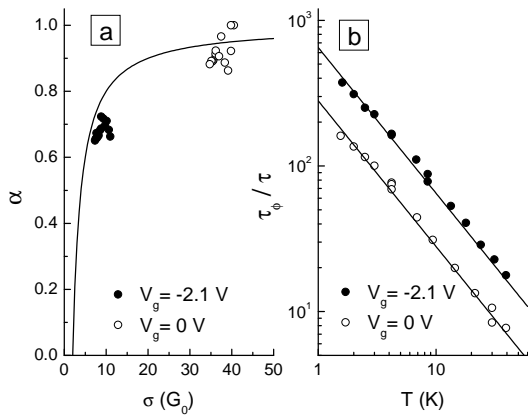


FIG. 3: (a) – The prefactor α as a function of conductivity varied with the temperature for $V_g = -2.1$ V and 0 V. Symbols are the data, solid line is Eq. (7). (b) – The temperature dependence of the τ_ϕ to τ ratio found experimentally from the shape of the magnetoconductance curve for $V_g = -2.1$ V and 0 V. Solid lines are the T^{-1} -law.

τ and B_{tr} using n obtained from the Hall measurements. Then, we have determined τ_ϕ/τ and α from the fit of experimental curve of magnetoconductance by the HLN-expression, Eq. (6). After that we have substituted the ratio τ_ϕ/τ into Eq. (4) and using experimental value of K_{ee} , Eqs. (5) and (3) found the corrected value of σ_0 (and, consequently, τ and B_{tr}). Found value of σ_0 was used for next step. A convergence of the procedure is good enough. It is sufficient to make from five to seven iterations to achieve an accuracy of several percent in the determination of σ_0 .

The values of σ_0 found in such a way for different temperatures are shown in Fig. 2(a) by solid circles. One can see that they are close to each other. This attests that (i) the model used is adequate, (ii) the value σ_0 found by this way is good estimate for the Drude conductivity. Thus, the Drude conductivity for the case of $V_g = -2.1$ V is equal to $\sigma_0 = (13.4 \pm 0.4) G_0$, that corresponds to $k_F l = 4.3 \pm 0.1$.

The parameters α and τ_ϕ/τ found from the processing of the magnetoconductivity curves are shown in Figs. 3(a) and 3(b), respectively. For completeness sake the results for $V_g = 0$ V are presented also. Note, the points in Fig. 3(a) for each gate voltage relate to the different temperatures. The parameter K_{ee} used for the estimate of interaction correction is equal here to 0.2 and 0.25 for $V_g = -2.1$ V and 0 V, respectively. As seen from Fig. 3(a) the conductivity dependence of the prefactor α is really close to the theoretical one, Eq. (7). The temperature dependence of the τ_ϕ to τ ratio is also close to that predicted theoretically,²² $\tau_\phi/\tau \propto 1/T$ [Fig. 3(b)].

As seen from Fig. 2(a) the temperature dependence of the conductivity at $B = 0$ accords with this model too. It is close to logarithmic with the slope $1 + 0.2$ where 1 and 0.2 come from WL and interaction corrections, respectively [dashed line in Fig. 2(a)].

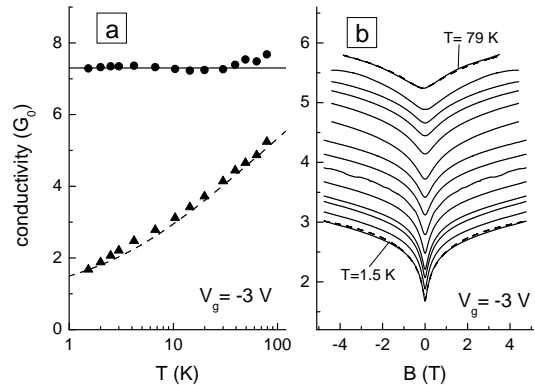


FIG. 4: (a) – The T -dependence of the conductivity at $B = 0$ measured for $V_g = -3$ V. The values measured experimentally shown as triangles. Circles are the Drude conductivity found experimentally for the different temperatures as described in text. The solid line is $\sigma_0 = 7.3 G_0$, the dashed line is Eq. (3) calculated with τ_ϕ^*/τ shown in Fig. 5(b), the dotted line the dependence $1.15 \ln T$. (b) – The magnetic-field dependence of the conductivity for different temperatures: $T = 79, 63, 49.2, 39.2, 30, 19.9, 14.4, 10.4, 6.7, 4.2, 3.0, 2.5, 2.0,$ and 1.5 K (from top to the bottom). Solid lines are experimental, dashed lines are the fit by Eq. (6) carried out within magnetic field range from $-0.3 B_{tr}$ to $0.3 B_{tr}$, $B_{tr} \simeq 3.1$ T.

Thus, all the temperature and magnetic field dependences of the conductivity for large enough $k_F l$ value are in quantitative agreement with the conventional theories of the quantum corrections, which take into account the two-loop interference correction and interplay between interference and interaction. We would like to emphasize here two important issues. First, the WL correction is dominant. For example, at $T = 1.6$ K $\delta\sigma^{WL} + \delta\sigma_b^{WL} \simeq -5.3 G_0$ while $\delta\sigma^{ee} \simeq -0.9 G_0$. Second, both corrections for such a strongly disordered systems significantly suppress the Drude conductivity already at large enough value of $k_F l$, $k_F l \simeq 4$.

Let us consider the results for stronger disorder. The temperature and magnetic field dependences of the conductivity at $V_g = -3$ V when $n = 8 \times 10^{11} \text{ cm}^{-2}$ are presented in Fig. 4. Again, the negative magnetoresistance is observed over the whole temperature range up to $T \simeq 80$ K. However, the variation of the conductivity with temperature remains close to $(1 + 0.15) \ln(T)$ (where 0.15 comes from interaction) only at $T > 10$ K and slackens noticeably at lower temperature. As well as in the previous case the magnetoresistance curves are well described by the HLN expression. The conductivity dependence of the prefactor α and the temperature dependences of the fitting parameter τ_ϕ^* are presented in Figs. 5(a) and 5(b), respectively (we asterisk here τ_ϕ because it is unknown in advance how the fitting parameter in the HLN-expression relates to the phase breaking time at low conductivity, $\sigma < e^2/h$). One can see that α decreases with the lowering conductivity and remains close to the theoretical dependence down to $\sigma \simeq 2.5 G_0$. The deviation at lower σ is not surprising because the

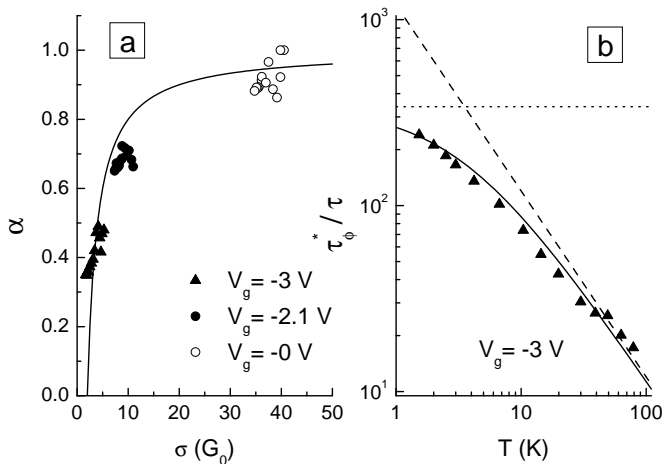


FIG. 5: (a) – The prefactor α as a function of the conductivity for the different gate voltages. Symbols are the data, solid line is Eq. (7). (b) – The temperature dependence of the τ_ϕ^* to τ ratio found experimentally for $V_g = -3$ V. The dashed line is $\tau_\phi/\tau = 1200/T$, the dotted line is $\tau_\xi/\tau = 340$, the solid line is $\tau_\phi^*/\tau = 1/(\tau/\tau_\phi + \tau/\tau_\xi)$.

theoretical dependence, Eq. (7), takes into account the first order in $1/\sigma$ -expansion only. The temperature dependence of τ_ϕ^* is close to theoretical $1/T$ -dependence only at $T > 20$ K and shows the tendency to saturation at lower temperature.

Before to consider possible reasons of the deviations of τ_ϕ^* -vs- T and $\sigma(B = 0)$ -vs- T dependences from that predicted by the conventional theories, let us evaluate the value of the Drude conductivity by the same way as in previous case. Using τ_ϕ^* as τ_ϕ in Eq. (4) and $K_{ee} = 0.15$ in Eq. (5), we obtain the results presented in Fig. 4(a) by solid circles. It is evident that the values of σ_0 found for different temperatures are close to each other that gives $\sigma_0 = (7.3 \pm 0.3) G_0$ and $k_F l = 2.3 \pm 0.1$. It should be stressed that $\beta = 1$ whereas $\alpha < 1$ in accordance with Ref. 21.

Now, we return to the saturation of the fitting parameter τ_ϕ^* with the decreasing temperature. Let us compare the two characteristic lengths: localization length ξ and the phase breaking length, $L_\phi = \sqrt{D\tau_\phi}$, where $D = \pi\hbar^2\sigma_0/(e^2m)$ is the diffusion coefficient. Using Eq. (1) we have $\xi \simeq 40l$ for $k_F l = 2.3$ found above. The L_ϕ value can be estimated under the assumption that the true phase breaking time τ_ϕ is inversely related to the temperature and can be obtained by extrapolating of the high-temperature data for τ_ϕ^* as shown in Fig. 5(b) by the dashed line. So, $\tau_\phi/\tau \simeq 1200/T$ for this case, that gives $L_\phi(T) \simeq 35l/T^{0.5}$. Thus, L_ϕ should become comparable with ξ at $T \sim 1$ K. To realize the consequences, recall that for fully delocalized electrons the increase of the magnitude of WL-correction with the temperature decrease results from the fact that the area contributing to the correction, which is proportional to L_ϕ^2 , linearly increases. It is naturally to suppose that when the

electron states becomes partially localized, i.e., $\xi \sim L_\phi$, the increasing of the interference correction at decreasing temperature is restricted not only by L_ϕ^2 but by ξ^2 also. Because of this, the effective area, which contributes to the interference correction, is $[(1/L_\phi)^2 + (1/\xi)^2]^{-1}$. In time domain this corresponds to introduction of the effective time τ_ϕ^* :

$$\tau_\phi^* = \left(\frac{1}{\tau_\phi} + \frac{1}{\tau_\xi} \right)^{-1}, \quad (8)$$

where $\tau_\xi = \xi^2/D$. How may this fact reveal itself in magnetoconductance? For large $k_F l$ -values, the shape of the magnetoconductance curve is determined by competition between L_ϕ and $l_H = \sqrt{\hbar/2eB}$. As for the considered case, the area which contributes to WL is restricted by $[(1/L_\phi)^2 + (1/\xi)^2]^{-1}$ instead of L_ϕ^2 and the shape of the magnetoconductance curve will give τ_ϕ^* instead of τ_ϕ .

As evident from Fig. 5(b) this simple model well describes the experimental τ_ϕ^* -vs- T dependence within whole temperature range if one supposes that $\tau_\xi/\tau = 340$ and $\tau_\phi/\tau = 1200/T$ in Eq.(8). The value of ξ found by this way, $\xi = \sqrt{D\tau_\xi} \simeq 19l$, somewhat differs from that estimated from Eq.(1), $\xi \simeq 40l$. Taking into account the qualitative character of our consideration these estimates can be viewed as consistent.

Thus, supposing that the conductivity is determined by delocalized states, as for large $k_F l$ -values, and the partial localization of the states leads only to restriction of the WL correction both by L_ϕ and by ξ , we are able to describe quantitatively all the experimental data, namely, the magnetoconductance, the temperature dependence of the conductivity at $B = 0$, and the temperature dependence of τ_ϕ^* .

Let us analyze the data with farther increasing of disorder. Figs. 6 and 7 show the temperature and magnetic dependences of the conductivity at $V_g = -3.4$ V, $n = 6.5 \times 10^{11}$ cm $^{-2}$. One can see that for this gate voltage the conductivity at highest temperature is large enough $\sigma(48.8$ K) $\simeq 2.4 G_0$. It strongly decreases with the lowering temperature and comprises only $0.038 G_0$ at $T = 0.42$ K. Usually, such a behavior of the conductivity is attributed with the crossover to the hopping regime. However, we direct reader's attention to the Hall effect. The transverse resistivity ρ_{xy} is linear with respect to magnetic field. The Hall density $n_H = 1/(eR_H)$ does not practically depend on the temperature (see the inset in Fig. 6) and gives correct density. This seems extraordinary for the hopping regime wherein the Hall effect is either absent or the value $1/(eR_H)$ has nothing to do with the carrier density.^{29,30,31,32}

So, the behavior of the Hall conductivity makes to believe that delocalized states determine the conductivity yet. Therefore, let us use the HLN expression for description of the negative magnetoconductance which is also observed over the whole temperature range [see Fig. 7(a)]. As in the above cases the experimental data are well described by the HLN expression [Fig. 7(b)]. The conduc-

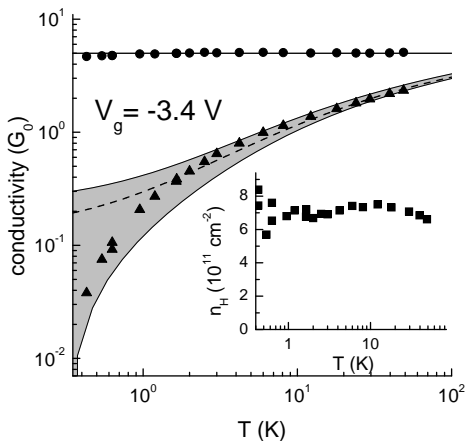


FIG. 6: The conductivity at $B = 0$ as a function of temperature for $V_g = -3.4$ V. The values measured experimentally shown as triangles. Circles are the Drude conductivity found experimentally for the different temperatures as described in text. Solid line is $\sigma_0 = 5.0 G_0$. Dashed line is Eq. (3) with τ_ϕ^*/τ shown in Fig. 8(b) by solid line. Dashed area is uncertainty in calculated $\sigma(T)$ caused by experimental error in determination of σ_0 and τ_ϕ^* . The inset shows the temperature dependence of the Hall electron density, $n_H = 1/(eR_H)$.

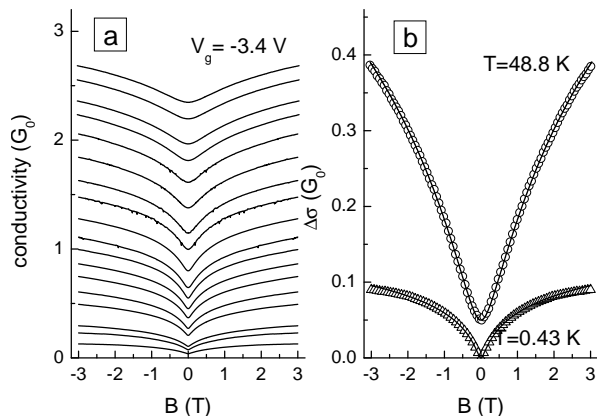


FIG. 7: (a) – The magnetic-field dependence of the conductivity measured at $V_g = -3.4$ V for different temperatures: $T = 48.8, 39.3, 29.5, 24.0, 18.0, 12.2, 8.1, 6.0, 4.2, 3.0, 2.5, 2.0, 1.64, 1.19, 0.95, 0.63, 0.54,$ and 0.43 K (from the top to bottom). (b) – The $\Delta\sigma$ -vs- B dependences for $V_g = -3.4$ V, $T = 48.8$ K and 0.43 K. Symbols are experimental data, lines are the fit by Eq. (6) carried out within magnetic field range from $-0.3 B_{tr}$ to $0.3 B_{tr}$, $B_{tr} = 5.3$ T. For clarity, the data for $T = 48.8$ K are shifted up by $0.05 G_0$.

tivity dependence of α and the temperature dependences of τ_ϕ^* are presented in Figs. 8(a) and 8(b), respectively. Again, if one calculates the Drude conductivity from the data measured at different temperatures using Eq.(3) ($K_{ee} = 0$ in this case), we obtain the values, which are practically independent of the temperature (see Fig. 6). Thus, we have $\sigma_0 \simeq 5.0 G_0$ and $k_F l \simeq 1.6$ in this case.

The temperature dependence of τ_ϕ^* shown in Fig. 8(b) is well described by Eq. (8) with $\tau_\xi = 260 l$ that gives

$\xi \simeq 16 l$. Note that this value is close to that found from Eq. (1), $\xi \simeq 12 l$.

What does happen at farther decreasing of the electron density?⁴³ The results for $V_g = -3.7$ V, $n = 5.2 \times 10^{11} \text{ cm}^{-2}$ are presented in Figs. 9, 10, and 11.

It is surprising, but the experimental temperature and magnetic field dependences of the conductivity remains analogous to that in the previous cases, the behavior of the fitting parameter of the magnetoconductivity τ_ϕ^* and α with temperature correlates quite well also. The only difference is that τ_ϕ^* starts to grow sharply at $T \lesssim 0.8$ K [Fig. 11(b)], when the conductivity becomes less than $10^{-2} G_0$. This occurs when $\tau_\phi \simeq 20 \tau_\xi$, i.e., the dephasing length L_ϕ is about five times larger than the localization length ξ . An important point is that the Hall effect is also measurable down to this temperature (see inset in Fig. 9). It is independent of the temperature, and $1/(eR_H)$ gives the electron density. It is impossible to measure the Hall effect for $T \lesssim 0.8$ K. Fluctuations of the odd in B voltage across the Hall probes are significantly larger in magnitude than the mean value of the voltage.

Thus, the analysis of the experimental data within wide temperature range, when both conditions $L_\phi < \xi$ and $L_\phi > \xi$ are realized, shows that the simple model of the conductivity over delocalized states well describes all the data when $\xi \gtrsim 0.2 L_\phi$. This model reduces to the following: there is the Drude conductivity; the main correction to it comes from the interference; the value of the interference contribution is $G_0 \ln(\tau/\tau_\phi + \tau/\tau_\xi)$; the value of τ_ϕ is proportional to $1/T$ over the whole range of the conductivity; the value of τ_ξ is $\sim \tau \exp(\pi k_F l)$; the magnetoresistance over the whole conductivity range is determined by suppression of the interference in the magnetic field; the σ -vs- B curve has the same shape as for the high conductivity, but it is controlled by $(\tau/\tau_\phi + \tau/\tau_\xi)$

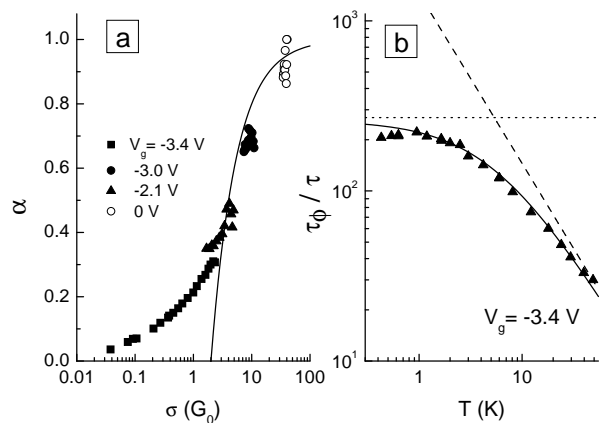


FIG. 8: (a) – The prefactor α as a function of conductivity for different gate voltages. Symbols are the data, the solid line is Eq. (7). (b) – The temperature dependence of the τ_ϕ to τ ratio found experimentally for $V_g = -3.4$ V. The dashed line is $\tau_\phi/\tau = 1450/T$, the dotted line is $\tau_\xi/\tau = 260$, the solid line is $\tau_\phi^*/\tau = 1/(\tau/\tau_\phi + \tau/\tau_\xi)$.

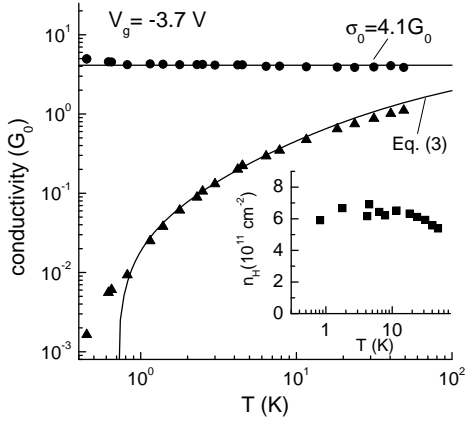


FIG. 9: The conductivity at $B = 0$ as a function of temperature for $V_g = -3.7$ V. The values measured experimentally shown as triangles. Circles are the Drude conductivity found experimentally for the different temperatures as described in text. The dashed line is calculated with $\Delta_\xi/\lambda = 14$ K. The inset shows the temperature dependence of the Hall electron density.

instead of τ/τ_ϕ ; the magnetoresistance has a prefactor that decreases with the lowering conductivity.

The dashed curves in panels (a) in Figs. 2, 4, 6, and 9 show how this model describes $\sigma(T)$ at $B = 0$. The curves have been calculated with σ_0 found above for each concrete case and with $1/\tau_\phi^*(T)$ shown by solid lines in panels (b) in Figs. 3, 5, 8, and 11. One can see that down to $\sigma \sim 0.01 G_0$ this simple model well describes the experimental data.

Thus, at low-temperature conductivity within the range ($10^{-1} - 10^{-2}$) G_0 which occurs at the Drude con-

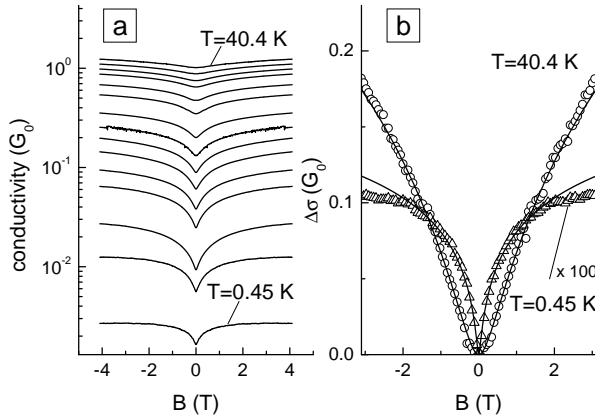


FIG. 10: (a) – The magnetic-field dependence of the conductivity measured at $V_g = -3.7$ V for different temperatures: $T = 40.4, 31.5, 23.7, 18.3, 11.6, 7.8, 4.2, 3.0, 2.3, 1.78, 1.39, 1.15, 0.82, 0.62,$ and 0.45 K. $B_{tr} = 6.3$ T. (b) – The $\Delta\sigma$ -vs- B dependences for $V_g = -3.7$ V, $T = 40.4$ K and 0.45 K. Symbols are experimental data, lines are the fit by Eq. (6) carried out within magnetic field range from $-0.3 B_{tr}$ to $0.3 B_{tr}$, $B_{tr} = 6.3$ T.

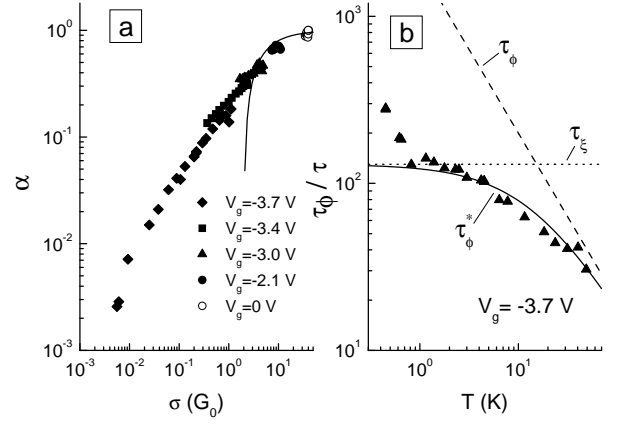


FIG. 11: (a) – The prefactor α as a function of conductivity for different gate voltages. Symbols are the data, the solid line is Eq. (7). (b) – The temperature dependence of the τ_ϕ to τ ratio found experimentally for $V_g = -3.7$ V. The dashed line is $\tau_\phi/\tau = 2000/T$, the dotted line is $\tau_\xi/\tau = 130$, the solid line is $\tau_\phi^*/\tau = 1/(\tau/\tau_\phi + \tau/\tau_\xi)$.

ductivity about $(4 - 5) G_0$ all the transport properties look like ones for the conductivity over delocalized states. However, it is clear that for the case when the interference correction becomes comparable with the Drude conductivity, the description of the system starting from “pure” states of the conduction band is inappropriate (see Fig. 6). It seems that another model of the charge transfer could be more suitable for this case. Namely, an electron can be considered as being localized within the area $\sim \xi^2$ during the time τ_ϕ . After this time, it leaves this area shifting by a some length L_i . Analogous model was considered in Refs. 33,34,35,36. It is natural to suppose that the length L_i should be shorter than the localization length ξ and longer than the mean distance between scatterers, $N_d^{-1/2}$: $\xi \gtrsim L_i \gtrsim N_d^{-1/2}$. Such a motion looks like the motion of delocalized electron with the diffusion coefficient $D \simeq L_i^2/\tau_\phi$ yielding the conductivity

$$\sigma(T) \simeq e^2 \nu \frac{L_i^2}{\tau_\phi(T)} = \frac{L_i^2}{l^2} \frac{\tau}{\tau_\phi(T)} \sigma_0, \quad (9)$$

where ν is density of the states.

To understand the soundness of the model, let us estimate the shifting length L_i . Using $\tau_\phi(T)/\tau$ shown for $V_g = -3.4$ V and -3.7 V by the dashed lines in Figs. 8(b) and 11(b), respectively, and the corresponding experimental T -dependences of σ from Figs. 6 and 9, we have found the length L_i as a function of temperature from Eq. (9) (see Fig. 12). One can see that the values of L_i are reasonable. They lie within the interval from $L_i \simeq 2 N_d^{-1/2} \simeq 0.3\xi$ at $\sigma \simeq 0.01 G_0$ (that corresponds to $V_g = -3.7$ V and $T = 0.8$ K) up to $L_i \simeq 8 N_d^{-1/2} \simeq 0.5\xi$ at $\sigma \simeq 0.5 G_0$ (that corresponds to $V_g = -3.4$ V and $T \simeq 1$ K). It seems natural that the Hall effect for this conductivity mechanism should exist and give the electron density. Unfortunately, this model was not elabo-

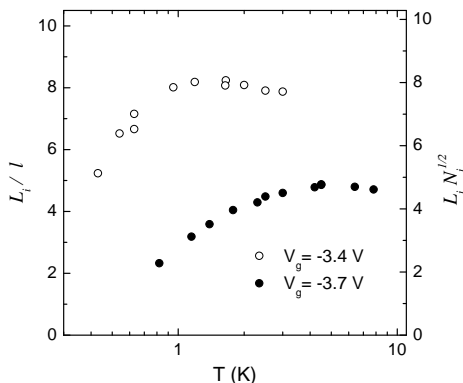


FIG. 12: The L_i to l ratio as a function of temperature for two gate voltages.

rated up to now and it makes no prediction about the magnetic field dependences of the conductivity or other effects.

IV. ANALYSIS FROM ALTERNATIVE STANDPOINTS

The conductivity of 2D systems is usually interpreted as the hopping one when it is less than e^2/h . Such consideration rests on a strong temperature dependence of the conductivity observed under this condition. This dependence for the different hopping mechanisms obeys the law

$$\sigma(T) = \sigma^0 \exp \left[- \left(\frac{T_0}{T} \right)^p \right], \quad (10)$$

where $p = 1$ for the nearest neighbor hopping, $p = 0.5$ or 0.3 for the variable range hopping (VRH) with the Coulomb gap or without it, respectively.

Additional argument is that the mean level spacing in localization length $\Delta_\xi = 1/(\nu\xi^2)$ becomes large than T . Really, the strong temperature dependence is observed in our case when $\sigma < e^2/h$ (see Figs. 6 and 9). The estimate of the mean level spacing, for example, for $V_g = -3.4$ V gives $\Delta_\xi \simeq 0.3 - 0.5$ meV $\simeq 4 - 6$ K. From the afore-said, it can mean that the probability of transition from one localized state to another becomes small already at $T \lesssim 4 - 6$ K, the states are well localized, and the conductivity is hopping. However, this estimation is very crude. The value Δ_ξ is the mean level spacing *within* the localization length, while the mean level spacing *between* the neighbor localized states, Δ_ξ^n , is of importance for the conductivity. Taking into account the fact that a localized state has a number of neighbors one can conclude that Δ_ξ^n should be several times less than Δ_ξ . Thus, we believe that the crossover to the hopping in the case considered has to be observed at the temperature, which is several times lower than Δ_ξ .

Let us inspect our data from the “hopping” point of view. Figure 13 shows the temperature dependences

of the conductivity at the different gate voltages $V_g \leq -3.4$ V when the conductivity becomes less than e^2/h . One can see that the data are well linearized in the coordinates $\ln \sigma$ -vs- T^{-p} with $p = 0.5$ within wide range of the temperature and conductivity. This were meant that one deals with the variable range hopping with the Coulomb gap.

Note, the most of the published data are also linearized in the VRH coordinates at $\sigma < e^2/h$. Practically all the authors present this fact as the main argument in favor the hopping mechanism of conductivity.^{12,13,15,16,18} Very wide range of the temperature and conductivity values, where the VRH law is observed, is reckoned as important argument *pro*. From our point of view it is argument *contra* rather than *pro*. Really, the equality $p = 0.5$ for our case might mean that the variable range hopping with the Coulomb gap is the main conductivity mechanism over the whole temperature range from 0.4 K up to 60 K. However, such a statement looks strange. Physically, it seems natural that the following conductivity regimes should change each other with the increasing temperature: the VRH with Coulomb gap ($p = 1/2$) \rightarrow the Mott law ($p = 1/3$) \rightarrow the nearest-neighbor hopping with $p = 1$ (the regime of so called ε_3 -conductivity). Finally, the transition (or crossover) to the conductivity over the delocalized states should happen. It seems that the variation of the temperature from $T \approx 0.04$ meV up to $T \approx 5$ meV should cover all these regimes, and the change both of the power p and of the characteristic temperature T_0 in the law given by Eq. (10) has to be observed experimentally.

The next strangeness of such “hopping” conductivity is the fact that the conductivity is well extrapolated at $T \rightarrow \infty$ to the value σ^0 , which is close to e^2/h . It is the value of the conductivity of one open channel. It seems that the conductivity between two localized states should be significantly lower. To interpret the high value of σ^0 , the new hopping mechanism, so called the electron-electron interaction assistant hopping, was proposed in Refs. 37 and 38. For the best of our knowledge there is not consistent theory for this hopping mechanism. In fact, it was found already in Ref. 39 that in the absence of phonons, the e - e interaction is not sufficient to support the variable range hopping in dimensionality $d < 3$, even for the case of long-range Coulomb interaction. This result was recently confirmed in Refs. 36 and 41.

Third, as already mentioned above the Hall effect is not measurable or the quantity $1/(eR_H)$ is not equal to the electron density for the case of conventional hopping conductivity.^{29,30,31,32} The insets in Figs. 6 and 9 show that the Hall coefficient in our experiment is independent of temperature, and Fig. 1(a) demonstrates that $1/(eR_H)$ gives the electron density.

All these features become transparent if one analyzes the data down to $\sigma \sim 10^{-2}G_0$ within the framework of the conductivity over delocalized states. First, the temperature dependences of the conductivity are consistently described within whole temperature range.

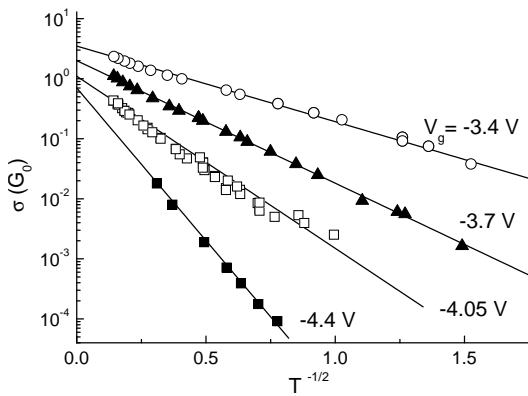


FIG. 13: The temperature dependence of the conductivity for different gate voltages plotted in the VRH coordinates. Symbols are the experimental results, lines are provided as a guide for the eye.

The second, the extrapolation of $\sigma(T)$ to e^2/h at $T \rightarrow \infty$ is absolutely natural because the strong temperature dependence of the conductivity is observed when the Drude conductivity is close to e^2/h . Therefore, independently of the manner, $\sigma(T)$ has to be extrapolated to the value close to e^2/h .

At last, the existence of the Hall effect, which gives the electron density, is natural for the conductivity over the delocalized states.

Thus, we believe that the hopping is inappropriate model for the description of the conductivity within the range $(1 - 10^{-2}) G_0$.

It may appear from reading of this and our previous papers that we deny the hopping conductivity mechanism in the 2D systems under investigation. This is not the case. As mentioned above the hopping between the nearest localized states, to our opinion, becomes to be the main conductivity mechanism when the conductivity becomes lower $\sim 10^{-2} G_0$. In this case the T -dependence of the conductivity should follow the law

$$\sigma(T) \simeq \sigma_3 \exp\left(-\frac{\varepsilon_3}{T}\right). \quad (11)$$

The experimental data for $V_g = -3.7$ V and -4.05 V are represented in Fig. 14 as $\lg \sigma$ -vs- T^{-1} plots in accordance with this point. One can really see that they approach exponential law, Eq. (11), with the decreasing temperature. As this takes place, the conductivity is less than $10^{-2} G_0$, therewith the value of σ_3 is significantly lower than e^2/h . The experimental activation energy ε_3 is 0.15 meV and 0.25 meV for the cases presented in Fig. 14. Let us compare these values with the mean level spacing Δ_ξ . The estimate for $V_g = -3.7$ V gives $\Delta_\xi \simeq 0.5$ meV and $\simeq 1$ meV depending on that what value of ξ , $\sqrt{D\tau_\xi}$ or $l \exp(\pi k_F l/2)$, we are using. For $V_g = -4.05$ V we, respectively, obtain $\Delta_\xi \simeq 0.7$ meV and $\simeq 1.5$ meV. The fact that the ε_3 -energy occurs three-seven times less than Δ_ξ is not surprising. As discussed in the beginning of this section the mean level spacing between the neighbor lo-

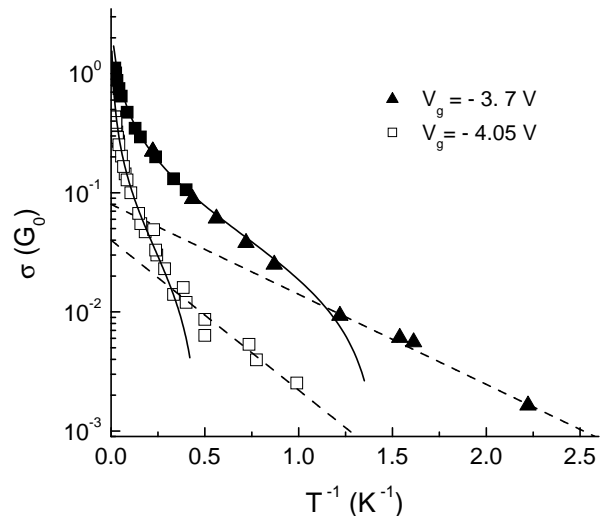


FIG. 14: The temperature dependence of the conductivity for two gate voltages, illustrating the crossover to the ε_3 -conductivity. Symbols are the experimental data, solid lines are drawn according to the model considered in Section III with $\sigma_0 = 4.1 G_0$, $\tau_\phi/\tau = 2000/T$, $\tau_\xi/\tau = 130$ for $V_g = -3.7$ V and $\sigma_0 = 3.4 G_0$, $\tau_\phi/\tau = 3800/T$, $\tau_\xi/\tau = 62$ for $V_g = -4.05$ V. The dashed lines are Eq. (11) with $\sigma_3 = 0.08 G_0$, $\varepsilon_3 = 0.15$ meV for $V_g = -3.7$ V and $\sigma_3 = 0.04 G_0$, $\varepsilon_3 = 0.25$ meV for $V_g = -4.05$ V.

calized states Δ_ξ^2 is of importance for the conductivity, rather than the mean level spacing within the localization length Δ_ξ which is essentially larger.

In Fig. 14, we present also the temperature dependences of the conductivity calculated within the framework of the model described in Section III. It is seen that the hopping regime matches the regime of the conductivity over the delocalized states quite well. The crossover happens when $\sigma \sim 10^{-2} G_0$.

All the above analysis was carried out within the model of single-particle localization. The e - e interaction was taken into account through the phase-breaking time only. Recently, the role of the many-body localization in the transport properties of low-dimensional systems was discussed in Refs. 40, 36, 41, and 42. It was shown that effects of Anderson localization in the many-body Fock space become efficient and dramatically suppress the direct current conductivity for $T \lesssim \Delta_\xi/\lambda$, where $\lambda^2 \ll 1$ is dimensionless coupling characterizing the e - e interaction, which is assumed to be short-range and weak. In particular, the many-body localization makes the variable-range hopping transport mechanism impossible in 2D in the absence of phonons.³⁹ The direct current conductivity should exactly vanish at finite low temperatures, in accordance with the prediction of Ref. 39; the corresponding characteristic critical temperature is given by $T_c \sim \Delta_\xi/(\lambda |\ln \lambda|)$. In Ref. 41 the stability of the metallic phase for $T \gg T_c$ and the insulating phase for $T \ll T_c$ was proved; the critical T -dependence of the conductivity in the vicinity of T_c was proposed in Ref. 36.

Since it is the value of λ^2 that determines the τ_ϕ -vs- T dependence, $\tau_\phi^{-1} \sim \lambda^2 T$, it can be easily estimated from the experimental data. For instance, we obtain $\lambda \simeq 0.4$ for $V_g = -3.7$ V using $\tau_\phi(T)$ shown in Fig. 11(b). With this value and $\Delta_\xi = 0.5 - 1$ meV, we have $T_c \simeq 15 - 30$ K (the very close results are obtained for other gate voltages). As evident from the above we observe no evidence of the critical behavior of σ at these temperatures as well as in the entire temperature range. (Actually, the expression for T_c may in principle contain numerical factors which would decrease the value of T_c by an order in magnitude as compared to the above estimate, see discussion in the beginning of this section).

Resuming this section we would like to underline that it is insufficient to analyze only the temperature dependence of the conductivity in order to establish the conductivity mechanism. It is necessary to know other theoretical predictions concerning, for example, the Hall effect, behavior of the conductivity in the magnetic and electric fields.

V. CONCLUSION

We have studied the temperature and magnetic field dependences of the conductivity in heavily doped, strongly disordered 2D quantum well structures within wide conductivity and temperature ranges. The role of interference in the temperature and magnetic field dependences has been traced when the phase breaking length controlled by the temperature occurs to be both larger and smaller than the localization length.

Our conclusions are pictorially summarized in Fig. 15 and accumulated in Table I. It has been shown that the four different areas, labeled as I – IV, can be fictionally distinguished in the T -dependence of the conductivity of 2D systems with different disorder strength. The boundaries between the areas are relatively smooth and shown in Fig. 15 approximately.

At $k_F l \gtrsim 4 - 5$ all the temperature and magnetic field dependences are in a good agreement with the conventional theories of the quantum corrections. This is area I. Here, inequality $\xi \gg L_\phi$ is fulfilled at any accessible temperatures.

At $k_F l \lesssim 4$ and $\sigma \gtrsim (2.5 - 3) G_0$, that corresponds to area II, the magnitude of the interaction correction tends to zero when $k_F l$ lowers. The low-magnetic-field magnetoconductivity caused by suppression of the interference quantum correction is described by the HLN-expression, Eq. (6), with the prefactor α , $\alpha \simeq 1 - 2G_0/\sigma$.

In the area III, the localization length ξ becomes comparable with the dephasing length L_ϕ . The interference contribution to the conductivity is now restricted not only by the phase breaking length L_ϕ , but by the localization length ξ as well. The quantity $(\tau_\phi^*)^{-1} = \tau_\phi^{-1} + \tau_\xi^{-1}$ rather than τ_ϕ^{-1} determines the behavior of the conductivity, $\tau_\phi \propto T^{-1}$ and $\tau_\xi \sim \tau \exp(\pi k_F l)$ therewith. The temperature dependence of the conductivity

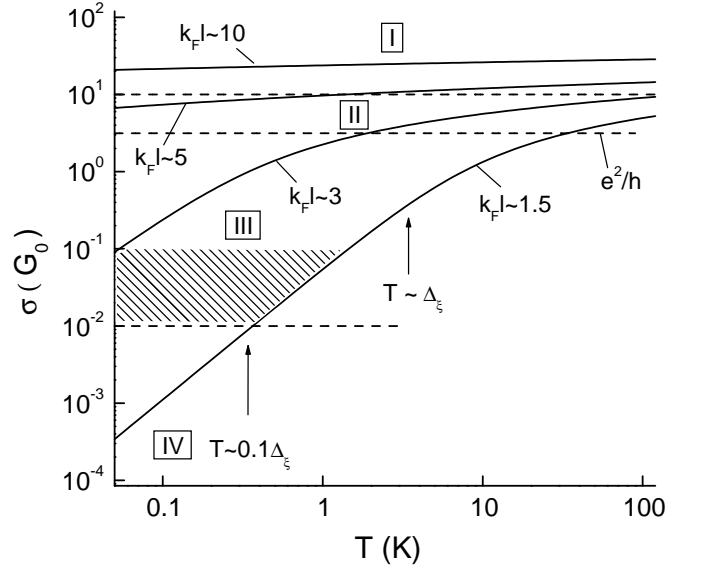


FIG. 15: The conductivity regimes in two-dimensions. Solid lines are the bulk-park temperature dependences of 2D disordered system with different $k_F l$ -values. The dashed lines conventionally demarcate the different areas (see text).

TABLE I: The T - and B -dependences of the conductivity for different areas shown in Fig. 15

Area	$\sigma(T, B=0)$	$\Delta\sigma(B)$
I	$\sigma_0 + \ln(\tau/\tau_\phi) + K_{ee} \ln T \tau$	$\alpha G_0 \mathcal{H}(\tau/\tau_\phi, B/B_{tr}),^a$ $\alpha = 1$
II	$\sigma_0 + \ln(\tau/\tau_\phi) + K_{ee} \ln T \tau$ $K_{ee} \rightarrow 0 @ k_F l \searrow$	$\alpha G_0 \mathcal{H}(\tau/\tau_\phi, B/B_{tr}),$ $\alpha = 1 - 2/\sigma$
III	$\sigma_0 + \ln(\tau/\tau_\phi + \tau/\tau_\xi)$ $\tau_\xi \sim \tau \exp(\pi k_F l)$	$\alpha G_0 \mathcal{H}(\tau/\tau_\phi + \tau/\tau_\xi, B/B_{tr}),$ $\alpha \rightarrow 0 @ \sigma \searrow$
IV	$\sigma_3 \exp(-\varepsilon_3/T)$ $\varepsilon_3 \simeq (0.1 - 0.3) \Delta_\xi$	determined by $\xi(B)$

^aThe function \mathcal{H} is defined in Eq. (6).

within this range can be well described by the formula $\sigma \simeq \sigma_0 + G_0 \ln(\tau/\tau_\phi^*)$ down to $\sigma \sim 10^{-2} G_0$. The magnetoconductivity is caused by suppression of the quantum interference. The σ -vs- B experimental plots are well described by the same formula, as in the weak-localization regime, Eq. (6), with τ_ϕ^* instead of τ_ϕ and with the prefactor, which value decreases with the lowering conductivity. This regime is realized in our temperature range when $k_F l \lesssim 2 - 3$ and $L_\phi \simeq (0.5 - 4) \xi$.

In the part of the area III shown by hatching in Fig. 15, in which $\sigma \sim (10^{-2} - 10^{-1}) G_0$, the other model considering the transport as the diffusion motion with $D \sim L_i^2/\tau_\phi$ ($\xi \gtrsim L_i \gtrsim N_d^{-1/2}$) could be more appropriate for description of the transport.

At last, when the temperature becomes 5 – 10 times

smaller than the mean level spacing in localization length Δ_ξ , the hopping between nearest neighbors becomes the main conductivity mechanism (area IV). For our case it occurs when the conductivity is less than $\sim 10^{-2} G_0$.

To our opinion, the scenario described is, in general, common for all disordered systems with two-dimensional gas of weak-interacting electrons ($r_s \lesssim 1$), in which spin-dependent processes are unimportant. Only the details, such as the temperature scale and the positions of the boundaries between areas, may be different for each concrete case.

Acknowledgment

We are grateful to Igor Gornyi for very useful discussions. This work was supported in part by the RFBR (Grant Nos. 04-02-16626, 05-02-16413, and 06-02-16292), and by a Grand from the President of Russian Federation for Young Scientists MK-1778.2205.2.

-
- ¹ E. Abrahams, P. W. Anderson, D. C. Licciardello, and T. V. Ramakrishnan, Phys. Rev. Lett. **42**, 673 (1979).
- ² P. A. Lee and T. V. Ramakrishnan, Rev. Mod. Phys. **57**, 287 (1985).
- ³ B. I. Shklovski and A. L. Efros, *Electronic Properties of Doped Semiconductors*, Springer Series in Solid-State Sciences (Springer-Verlag, New York, 1984).
- ⁴ E. Abrahams, S. V. Kravchenko, and M. P. Sarachik, Rev. Mod. Phys. **73**, 251 (2001).
- ⁵ B. L. Altshuler, D. L. Maslov, and V. M. Pudalov, Physica E **9**, 209 (2001).
- ⁶ S. Hikami, A. I. Larkin, and Y. Nagaoka, Prog. Theor. Phys. **63**, 707 (1980).
- ⁷ A. Kawabata, J. Phys. Soc. Jpn **53**, 3540 (1984).
- ⁸ H.-P. Wittmann and A. Schmid, J. Low Temp. Phys **69**, 131 (1987).
- ⁹ W. Knap, A. Zduniak, L. H. Dmowski, S. Contreras, and M. I. Dyakonov, Phys. Stat. Sol. (b) **198**, 267 (1996).
- ¹⁰ A. Zduniak, M. I. Dyakonov, and W. Knap, Phys. Rev. B **56**, 1996 (1997).
- ¹¹ A. P. Dmitriev, V. Y. Kachorovskii, and I. V. Gornyi, Phys. Rev. B **56**, 9910 (1997).
- ¹² F. W. V. Keuls, X. L. Hu, H. W. Jiang, and A. J. Dahm, Phys. Rev. B **56**, 1161 (1997).
- ¹³ F. W. V. Keuls, H. Mathur, H. W. Jiang, and A. J. Dahm, Phys. Rev. B **56**, 13263 (1997).
- ¹⁴ M. V. Budantsev, Z. D. Kvon, A. G. Pogosov, G. M. Gusev, J. C. Portal, D. K. Maude, N. T. Moshegov, and A. I. Toropov, Physica B: Condensed Matter **258**, 595 (1998).
- ¹⁵ I. Shlimak, S. I. Khondaker, M. Pepper, and D. A. Ritchie, Phys. Rev. B **61**, 7253 (2000).
- ¹⁶ M. E. Gershenson, Y. B. Khavin, D. Reuter, P. Schafmeister, and A. D. Wieck, Phys. Rev. Lett. **85**, 1718 (2000).
- ¹⁷ G. M. Minkov, O. E. Rut, A. V. Germanenko, A. A. Sherstobitov, B. N. Zvonkov, E. A. Uskova, and A. A. Birukov, Phys. Rev. B **65**, 235322 (2002).
- ¹⁸ F. E. Camino, V. V. Kuznetsov, E. E. Mendez, M. E. Gershenson, D. Reuter, P. Schafmeister, and A. D. Wieck, Phys. Rev. B **68**, 073313 (2003).
- ¹⁹ M. E. Gershenson, Y. B. Khavin, A. G. Mikhalechuk, H. M. Bozler, and A. L. Bogdanov, Phys. Rev. Lett. **79**, 725 (1997).
- ²⁰ Y. B. Khavin and M. E. Gershenson, Phys. Rev. B **58**, 8009 (1998).
- ²¹ G. M. Minkov, A.V.Germanenko, and I.V.Gornyi, Phys. Rev. B **70**, 245423 (2004).
- ²² B. L. Altshuler and A. G. Aronov, *Electron-electron interaction in disordered conductors*. in Electron-Electron Interaction in Disordered Systems, Edited by A. L. Efros and M. Pollak (North Holland, Amsterdam, 1985).
- ²³ A. M. Finkelstein, Zh. Éksp. Teor. Fiz. **84**, 168 (1983) [Sov. Phys. JETP **57**, 97 (1983)]; Z. Phys. B: Condens. Matter **56**, 189 (1984).
- ²⁴ C. Castellani, C. D. Castro, P. A. Lee, and M. Ma, Phys. Rev. B **30**, 527 (1984).
- ²⁵ C. Castellani, C. D. Castro, M. Ma, and P. A. Lee, Phys. Rev. B **30**, 1596 (1984).
- ²⁶ C. Castellani, C. D. Castro, and P. Lee, Phys. Rev. B **57**, R9381 (1998).
- ²⁷ G. M. Minkov, O. E. Rut, A. V. Germanenko, A. A. Sherstobitov, V. I. Shashkin, O. I. Khrykin, and B. N. Zvonkov, Phys. Rev. B **67**, 205306 (2003).
- ²⁸ I. L. Aleiner, B. L. Altshuler, and M. E. Gershenson, Waves in Random Media **9**, 201 (1999).
- ²⁹ L. Friedman and M. Pollak, Philos. Mag. B **38**, 173 (1978).
- ³⁰ L. Friedman, Philos. Mag. B **38**, 467 (1978).
- ³¹ D. C. Look, D. C. Walters, M. O. Manasreh, J. R. Sizelove, C. E. Stutz, and K. R. Evans, Phys. Rev. B **42**, 3578 (1990).
- ³² C. E. Nebel, M. Rother, M. Stutzmann, C. Summonte, and M. Heintze, Philos. Mag. Lett. **74**, 455 (1996).
- ³³ A. A. Gogolin, V. I. Melnikov, and E. I. Rashba, Zh. Eksp. Teor. Fiz. **69**, 327 (1975) [Sov. Phys. JETP **42**, 168 (1975)].
- ³⁴ D. J. Thouless, Phys. Rev. Lett. **39**, 1167 (1977).
- ³⁵ A. A. Gogolin and G. T. Zimányi, Solid State Commun. **46**, 469 (1983).
- ³⁶ I. V. Gornyi, A. D. Mirlin, and D. G. Polyakov, Phys. Rev. Lett. **95**, 206603 (2005).
- ³⁷ V. I. Kozub, S. D. Baranovskii, and I. Shlimak, Solid State Commun. **113**, 587 (2000).
- ³⁸ I. Shlimak and M. Pepper, Phil. Mag. B **81**, 1093 (2001).
- ³⁹ L. Fleishman and P. W. Anderson, Phys. Rev. B **21**, 2366 (1980).
- ⁴⁰ I. V. Gornyi, A. D. Mirlin, D. G. Polyakov, cond-mat/0407305v1 (unpublished).
- ⁴¹ D. M. Basko, I. L. Aleiner, and B. L. Altshuler, Annals of Physics **321**, 1126 (2006).
- ⁴² D. M. Basko, I. L. Aleiner, B. L. Altshuler, cond-mat/0602510 (unpublished).
- ⁴³ The decreasing of electron density can lead to that the Fermi level turns out below the classical mobility edge. The study of the capacitance-voltage characteristics for our samples shows that it is not the case.